



An examination of the vibration transmissibility of the hand-arm system in three orthogonal directions



Daniel E. Welcome, Ren G. Dong^{*}, Xueyan S. Xu, Christopher Warren,
Thomas W. McDowell, John Z. Wu

Engineering & Control Technology Branch, National Institute for Occupational Safety and Health, 1095 Willowdale Road, Morgantown, WV 26505, USA

ARTICLE INFO

Article history:

Received 21 May 2012

Received in revised form

11 July 2014

Accepted 22 November 2014

Available online 13 December 2014

Keywords:

Hand-arm vibration transmissibility

Hand-transmitted vibration

Human-arm vibration

Vibration biodynamic response

ABSTRACT

The objective of this study is to enhance the understanding of the vibration transmission in the hand-arm system in three orthogonal directions (X, Y, and Z). For the first time, the transmitted vibrations distributed on the entire hand-arm system exposed in the three orthogonal directions via a 3-D vibration test system were measured using a 3-D laser vibrometer. Seven adult male subjects participated in the experiment. This study confirms that the vibration transmissibility generally decreased with the increase in distance from the hand and it varied with the vibration direction. Specifically, to the upper arm and shoulder, only moderate vibration transmission was measured in the test frequency range (16 to 500 Hz), and virtually no transmission was measured in the frequency range higher than 50 Hz. The resonance vibration on the forearm was primarily in the range of 16–30 Hz with the peak amplitude of approximately 1.5 times of the input vibration amplitude. The major resonance on the dorsal surfaces of the hand and wrist occurred at around 30–40 Hz and, in the Y direction, with peak amplitude of more than 2.5 times of the input amplitude. At higher than 50 Hz, vibration transmission was effectively limited to the hand and fingers. A major finger resonance was observed at around 100 Hz in the X and Y directions and around 200 Hz in the Z direction. In the fingers, the resonance magnitude in the Z direction was generally the lowest, and the resonance magnitude in the Y direction was generally the highest with the resonance amplitude of 3 times the input vibration, which was similar to the transmissibility at the wrist and hand dorsum. The implications of the results are discussed.

Relevance to industry: Prolonged, intensive exposure to hand-transmitted vibration could result in hand-arm vibration syndrome. While the syndrome's precise mechanisms remain unclear, the characterization of the vibration transmissibility of the system in the three orthogonal dimensions performed in this study can help understand the syndrome and help develop improved frequency weightings for assessing the risk of the exposure for developing various components of the syndrome.

Published by Elsevier B.V.

1. Introduction

Hand-transmitted vibration exposure is associated with hand-arm vibration syndrome (HAVS) (NIOSH, 1997; Griffin, 1990). Although many studies on this subject have been reported, the syndrome's precise mechanisms remain unclear (ISO 5349-1, 2001). One of the essential foundations for further understanding their mechanisms is the biodynamic responses of the hand-arm system to vibration (Griffin, 1994; Dong et al., 2005a, b). Because

the transmissibility on the human body is directly measurable, it can be used to represent the distributed features of the system responses, and it has a certain relationship with the driving-point response function (Dong et al., 2013), the examination of the vibration transmissibility has been used as one of the major approaches to quantify and understand the biodynamic responses.

It remains a challenging task to accurately measure the transmitted vibration on the hand-arm system of a subject. While no feasible non-invasive method has been developed to measure the vibration inside the system of a human subject, the measurement has been most frequently performed at the surface of the hand-arm system using miniature accelerometers (Pyykkö et al., 1976; Reynolds 1977; Griffin et al., 1982; Gurram et al., 1994; Cherian et al., 1996; Thomas and Beauchamp, 1998; Adewusi et al., 2012).

^{*} Corresponding author. ECTB/HELD/NIOSH/CDC, 1095 Willowdale Road, MS L-2027, Morgantown, WV 26505, USA. Tel.: +1 304 285 6332; fax: +1 304 285 6265.
E-mail address: rkd6@cdc.gov (R.G. Dong).

The attachment of an accelerometer to the skin usually introduces some artificial constraints to the local structure where the vibration is measured. The mass of the accelerometer could also significantly affect the measurement results. This is primarily because the resonant frequency of the mass-skin assembly is likely to be within the frequency range of concern for hand-transmitted vibration exposure. A tight fixation may increase the attachment stiffness so that the useful measurement frequency range can be increased; however, this may further alter the biodynamic properties of the local structure. These effects also make it impractical to attach a sufficient number of accelerometers on the system to characterize the vibration distribution with reasonable spatial resolution. Furthermore, it is very difficult to fix and determine the global orientation of the accelerometer at each measurement location, because the orientation of the accelerometer fixed on the deformable contact surface may vary with the applied force and pressure distribution, which may also vary with subject and measurement location.

These problems can be largely overcome by using a three-dimensional (3-D) laser vibrometer. While a 1-D laser vibrometer has been used for the measurement of the transmitted vibration in the direction approximately vertical to the surface of the hand-arm system (Sörensson and Lundström, 1992; Rossi and Tomasini, 1995; Deboli et al., 1999; Nataletti et al., 2005; Scalise et al., 2007; Concettoni and Griffin, 2009; Xu et al., 2011), the feasibility of applying a 3-D laser vibrometer to reliably measure multi-axial vibrations of the hand-arm system has not been proven. Except for a preliminary introduction of the current study (Welcome et al., 2011), the application of a 3-D laser vibrometer for the measurement of 3-D vibrations on the entire hand-arm system was not found during the literature review for this study.

The reported transmissibility data, together with the driving-point response functions, have provided a general understanding of the vibration transmission in the hand-arm system, especially along the forearm direction. Specifically, the vibration can be effectively transmitted to the head, neck, shoulder, and/or arms below 25 Hz (Pyykkö et al., 1976; Sakakibara et al., 1986; Reynolds, 1977). This explains why the low-frequency vibration is predominantly perceived in these substructures (McDowell et al., 2007). This also partially explains why the most highly weighted frequencies for subjective sensation or discomfort for the hand-transmitted vibration exposure are in the low frequency range (Miwa, 1968; Giacomini et al., 2004; Morioka and Griffin, 2006). While the major resonance of the shoulder and upper arm is likely to be in the range of 8–12 Hz (Kinne et al., 2001; Dong et al., 2007; Adewusi et al., 2012), the major wrist-forearm resonance is usually in the range of 16–40 Hz (Thomas and Beauchamp, 1998; Kihlberg et al., 1995; Dong et al., 2007, 2012). Above 100 Hz, the vibration transmission is largely limited to the hand and fingers (Pyykkö et al., 1976; Reynolds, 1977). The major finger resonance can vary from 80 to more than 300 Hz (Sörensson and Lundström, 1992; Dong et al., 2007), depending on the specific locations on the fingers and the applied finger forces.

There are large differences among the impedance data measured in different directions (Dong et al., 2012). This suggests that the vibration transmission in the hand-arm system should also vary significantly with the vibration directions. However, their specific differences have not been clearly identified. It is common knowledge that the stiffness of the human skin in the shear or tangential direction under pressure is usually much less than that in the compression direction. The low stiffness could significantly reduce the useful measurement frequency range in the directions tangential to the skin using conventional accelerometers, casting some doubt on the reported data. However, little information on the vibration transmissibility in the tangential directions was

available from the reported studies that used the 1-D laser vibrometer in the measurement. Furthermore, the vast majority of the reported studies did not measure or report the phase angle of the transmissibility, which often proves useful, for example to determine the phase relationships among the vibration motions at different locations or the vibration mode shapes of the system. Simultaneous measurement of 3-D vibration transmissibility will also provide coupled 3-D vibration transfer functions of the system, which will be essential to develop a more realistic 3-D model of the hand-arm system but this has not been yet attempted.

Based on this background, the specific aims of this study are twofold: (a) to examine the feasibility of using a 3-D laser vibrometer for the measurement of the 3-D transfer functions on the hand-arm system; and (b) to characterize the vibration transfer functions distributed on the entire hand-arm system in three orthogonal directions. The implications of the results for developing improved biodynamic models of the system are also discussed.

2. Method

2.1. Experimental setup

Seven healthy male adults participated in this study. Their anthropometric measurements are listed in Table 1. The study protocol was reviewed and approved by the NIOSH Human Subjects Review Board.

Fig. 1 shows the basic instrumentation setup and the subject posture. A pictorial view of the setup is shown in Fig. 2. A 3-D vibration test system (MB Dynamics, 3-D Hand-Arm Vibration Test System) was employed to generate the required vibration spectra in three directions: Z - along the forearm; Y - along the centerline of the instrumented handle in the vertical direction; and X - in the horizontal plane normal to the Y-Z plane. An instrumented handle equipped with a tri-axial accelerometer (ENDEVCO 65–100) and a pair of 3-D force sensors (Kistler 9017B and 9018B) was used to measure the accelerations and applied grip force in three directions. A force plate (Kistler 9286AA) was used to measure the push force applied to the handle. Each subject was also instructed to grip the handle with the forearm parallel to the floor and aligned with the Z axis, the elbow angled between 90° and 120°, and shoulder abducted between 0° and 30°; these parameters are similar to those recommended in the standardized glove test (ISO 10819, 1996) and those used for the reference values in ISO-10068 (1998). As also used in these standards, 30 N grip and 50 N push are generally considered as the average hand forces applied in many tool operations. Therefore, the grip and push forces were also controlled as 30 ± 5 N and 50 ± 8 N, respectively, in the current study. The measured forces were displayed on two virtual dial gauges on a computer monitor in front of the subject, as also shown

Table 1
Subject anthropometry (hand length = tip of middle finger to crease at wrist; hand breadth = the width measured at metacarpal).

Subject	Height (cm)	Weight (kg)	Hand length (mm)	Hand breadth (mm)
1	180.8	80.70	200	90
2	185.4	69.10	192	86
3	182.9	68.95	192	84
4	176.5	79.83	193	83
5	180.3	88.45	192	89
6	179.1	87.00	190	89
7	181.6	99.79	200	94
Mean	180.9	81.97	194	88
SD	2.8	11.00	4	4

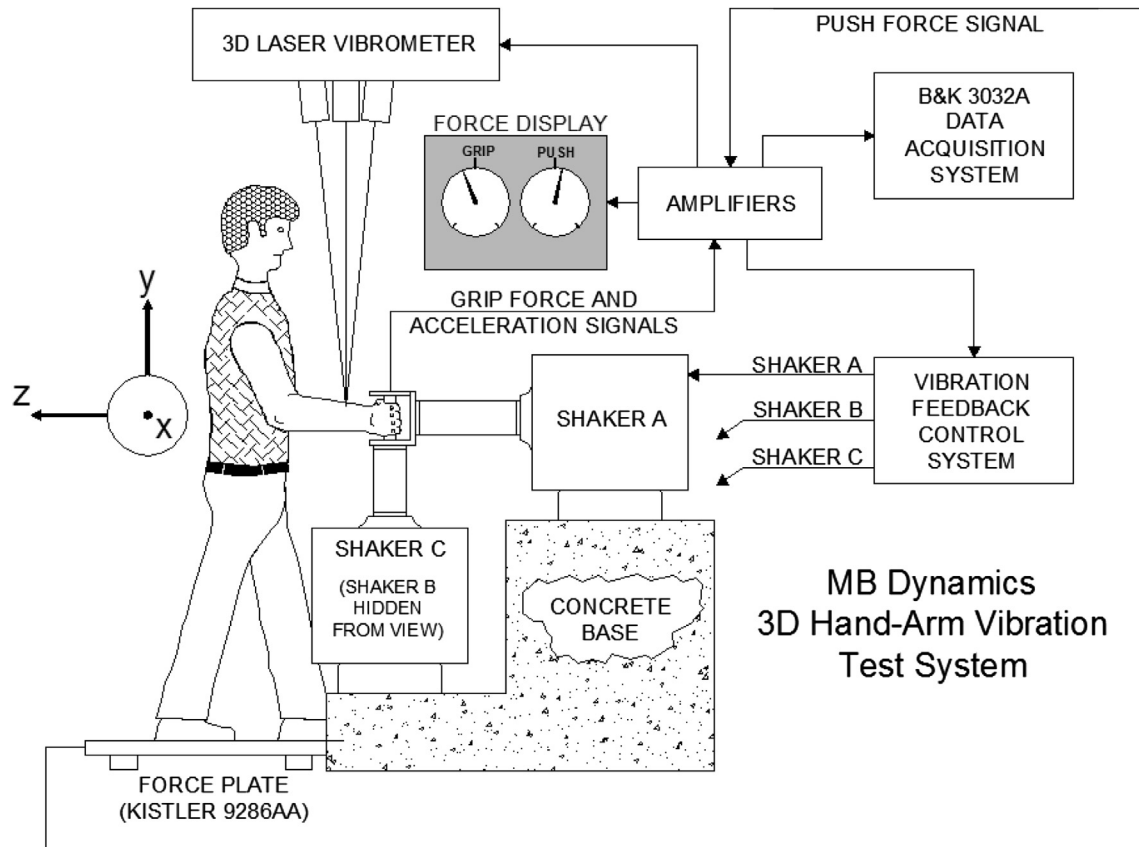


Fig. 1. Subject and measurement set-up that includes a closed-loop controlled vibration excitation system, a 3-D laser vibrometer, a vibration and response measurement system, a grip force measurement and display system, and a push force measurement and display system.

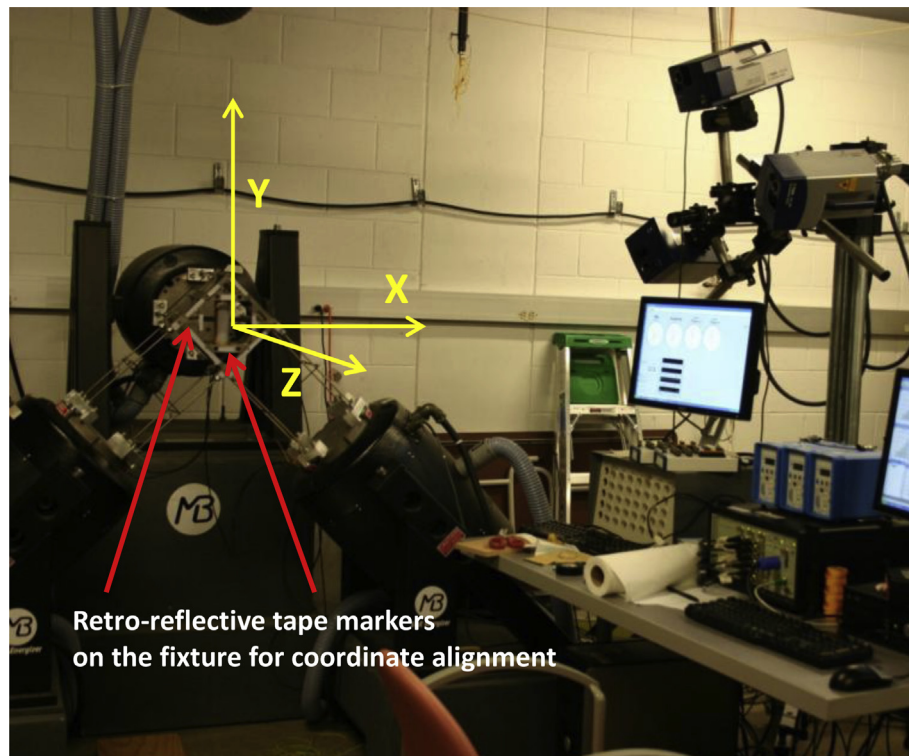


Fig. 2. A pictorial view of the 3-D laser vibrometer.

in Fig. 1. A broadband random vibration from 16 to 500 Hz was used as the excitation in each direction, which was the same as used in a reported study (Welcome et al., 2014). The overall root-mean-square value of the acceleration in each direction was 19.6 m/s^2 . All vibration signals were input to the data acquisition system of the laser vibrometer, and the vibration transfer function was evaluated using the cross-axis function built in the data processing program of the vibrometer. The signals from the tri-axial accelerometer installed in the handle were also input to a data acquisition system (B&K, 3032A) to monitor the controlled vibration in each direction.

A 3-D scanning laser vibrometer (Polytec, PSV-400-3D) was used to measure the distributed 3-D vibrations on the surface of the instrumented handle and on the skin of the hand-arm system, as shown in Fig. 2. The 3-D laser vibrometer is composed of three single-axis laser units positioned at three different positions and angles. The three laser beams are focused as close as possible on the same point to provide an accurate measurement. The reflected laser signal from the object surface is detected by each unit and input to the data acquisition system of the 3-D vibrometer to determine the vibration in each direction of the vibrometer coordinate system. Before the measurement, the 3-D laser coordinate system was aligned with the coordinate system of the 3-D vibration test system, which were marked on the fixture of the instrumented handle (see Figs. 2 and 3). The 3-D laser vibrometer was operated by a very experienced engineer from the laser vibrometer manufacturer during the entire experiment of the study.

To assure the validity of the 3-D instrumented handle and the 3-D laser vibrometer used in the measurement, this study performed a series of evaluation experiments prior to the subject tests. The vibration transmissibility of the hand-contact area on the instrumented handle in the three directions was measured using both the 3-D laser vibrometer and a 1-D laser vibrometer (Polytec, H-300). If their results in each direction are consistent, the 3-D laser measurement should be considered valid, as the 1-D laser vibrometer has been sufficiently validated. The handle surface transmissibility was also used as a baseline for the correction of the raw data measured in the subject tests, which is further elaborated in Section 2.3.

2.2. Subject testing procedures

The study and subject testing procedures were explained to each subject upon arrival. After signing the required consent form, the subject practiced the grip and push actions in the postures shown in Figs. 1 and 3. Because it was impossible to cover the full range of the hand-arm system in the field of view of the laser vibrometer, the measurement was divided into four areas, with each area focused on one of the four substructures: fingertip area (Fig. 4), proximal finger area (Fig. 4), hand dorsum area (Fig. 5), and wrist-forearm-upper arm area (Fig. 3). While the measurements on the fingers and arm were performed with the regular postures shown in Figs. 1 and 3, a special posture was used to measure the transmissibility on the dorsal hand, as shown in Fig. 5. This was because the handle fixture blocked part of the hand surface holding the handle. For the same reason, the transmissibility on the fingers could be measured only at very limited locations. Similar to the technique used by Sörensson and Lundström (1992), sections of retro-reflective tape were used in the measurement in order to avoid the effect of hair on the measurement and to provide improved laser reflection, which is also shown in Figs. 3–5. To avoid any adverse effects of the retro-reflective tape on the subject skin, first-aid adhesive tape was placed between the reflecting tape and the skin, which also assured a firm attachment of the reflecting tape on the skin.

After the subject was comfortable performing the required actions and stably maintaining the required grip and push forces, the laser vibrometer started to scan the vibrations at each defined location. The measurement process for each trial usually took less than 3 min, primarily depending on the number of scanning points in each measurement area. Ideally, the laser beam should be focused at a single point at each measuring location. This was, however, very difficult to achieve in the human subject test, partially because of the limitations of the 3-D vibrometer, and partially because of the difficulty to maintain a very stable and precise position of the hand-arm system. As a result, in many instances, the three laser beams could not be precisely focused at the same point, but they were controlled to within the taped area at

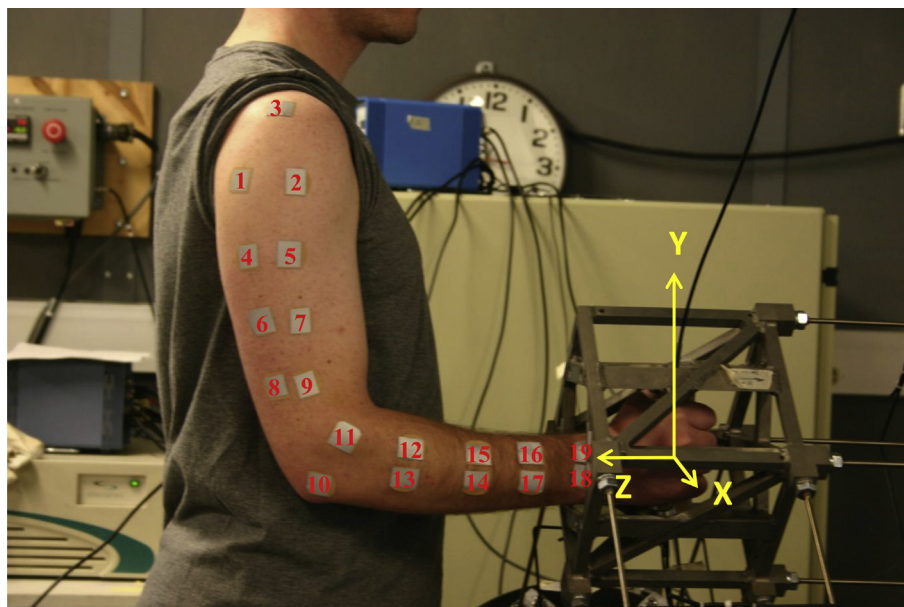


Fig. 3. A pictorial view of the instrumented handle and its fixture on the 3-D hand-arm vibration test system, together with a test subject with nineteen pieces of reflecting tape attached at the measuring points on the arms.

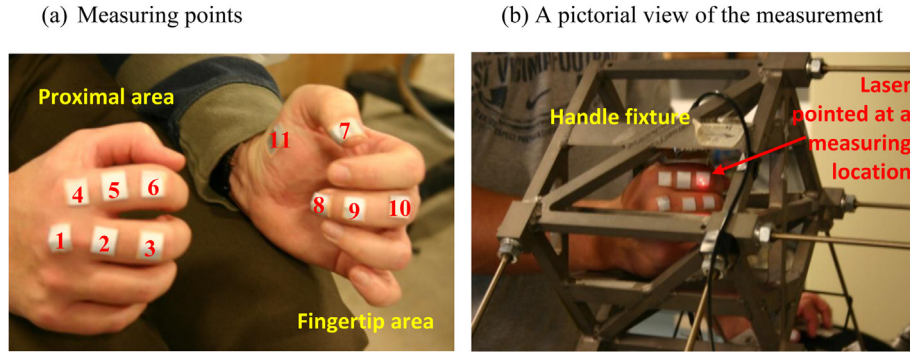


Fig. 4. Measurement locations on the fingers on the two hands and a pictorial view of the right hand holding the handle in the measurement.

each measuring location, as shown in Fig. 4. Because it is more difficult to control the arm position than to control the hand position, the size of each piece of reflecting tape on the arms ($\approx 3 \text{ cm}^2$) was larger than that on the fingers and the dorsal hand ($\approx 1 \text{ cm}^2$). After each trial, the subject rested for at least 2 min before the next trial. Two consecutive trials were performed for each measurement area. Each subject completed eight trials for the measurements in the four areas. The orders of the measurement areas were randomly arranged among the subjects.

2.3. Calculation of the vibration transmissibility

The laser vibrometer directly measures the vibration velocity, so the measured data were converted into acceleration using the program built in the laser vibrometer's data acquisition system. Then, the transmissibility (T_{Handle}) in each direction (i) from the accelerometer installed in the handle to the handle surface is calculated using the following formula:

$$T_{\text{Handle}_i}(\omega) = \frac{A_{\text{Handle}_i}(\omega)}{A_{\text{Acc}_i}(\omega)}; \quad i = X, Y, \text{ and } Z, \quad (1)$$

where A_{Handle} is the acceleration of the handle surface measured with the laser vibrometer, A_{Acc} is the acceleration measured using the accelerometer, and ω is the vibration frequency in rad/sec.

Similarly, the raw transmissibility measured at a point on the skin of the hand-arm system (T_{Raw}) is calculated using the following formula:

$$T_{\text{Raw}_i}(\omega) = \frac{A_{\text{Hand-Arm}_i}(\omega)}{A_{\text{Acc}_i}(\omega)}; \quad i = X, Y, \text{ and } Z, \quad (2)$$

where $A_{\text{Hand-Arm}}$ is the acceleration measured on the skin using the laser vibrometer. The two transmissibility functions were expressed in the equal frequency bands with increments of 1.25 Hz.

The raw transmissibility calculated using Eq. (2) actually includes the transmissibility of the handle and accelerometer, which can be eliminated. By definition, the transmissibility of the hand-arm system ($T_{\text{Hand-Arm}}$) is derived as follows:

$$T_{\text{Hand-Arm}} = \frac{A_{\text{Hand-Arm}}}{A_{\text{Handle}}} = \frac{A_{\text{Hand-Arm}}}{A_{\text{Acc}}} \cdot \frac{A_{\text{Acc}}}{A_{\text{Handle}}} = \frac{T_{\text{Raw}}}{T_{\text{Handle}}} \quad (3)$$

2.4. Statistical analyses

The two repeated trials under each condition were utilized for the statistical analysis. As it is well understood that the transmissibility is a function of vibration frequency, general linear model analyses of variance (ANOVA) tests of vibration transmissibility were performed to identify the significance of the following fixed factors: direction and measuring location. Subject was treated as a random factor. The ANOVAs were performed using MINITAB statistical software (version 13.1). Differences were considered significant at the $p < 0.05$ level.

3. Results

3.1. Evaluation of the 3-D laser vibration measurement

Fig. 6 shows transfer functions obtained in the measurements of the handle 3-D vibrations using the 1-D and 3-D laser vibrometers. The 3-D results indicate that the handle surface responses in the three directions are very similar. The magnitudes at most

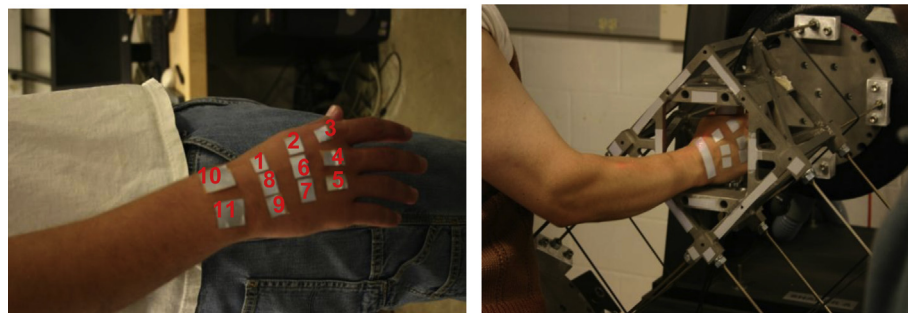


Fig. 5. Measurement locations on the hand dorsum and a pictorial view of the hand-arm posture in the measurement. The arms had to take an angle from the original forearm direction and the forearm could slightly touch the corner edges of the handle fixture so that the three laser beams could reach each measuring point on the hand dorsum.

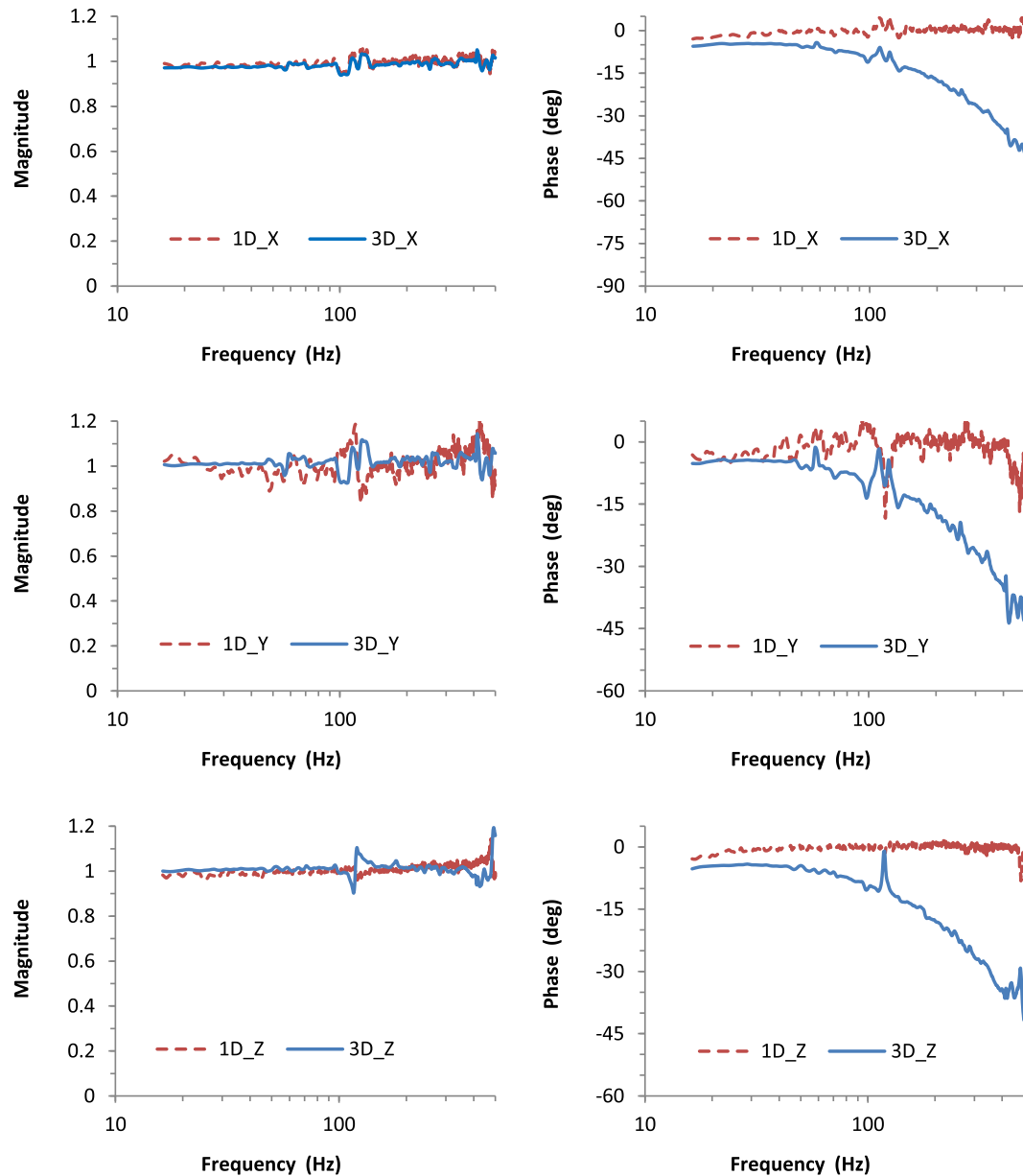


Fig. 6. Handle surface transmissibility functions in three orthogonal directions measured using 1-D laser vibrometer and 3-D laser vibrometer.

frequencies in the entire range (16–500 Hz) are fairly constant (difference < 5%). There is a small resonance near 110 Hz and a slightly bigger resonance at around 400 Hz. The magnitudes measured with the 1-D laser vibrometer were generally consistent with those measured by the 3-D laser vibrometer in the X and Z directions. This was because they were measured at the same locations on the handle. However in the Y direction, it was impossible to measure the vibration at the same locations on the handle because the measured surface must be approximately vertical to the laser beam of the 1-D laser vibrometer, and these locations were blocked by the fixture frames (Fig. 3); therefore the 1-D laser beam could not reach the handle surface in its measurable angle range. Alternatively, the measurement in the Y direction was performed on the frame of the handle fixture with the assistance of a single-surface mirror suspended above the fixture. As expected, the results in the Y are more different because the response on the frame is somewhat different from that on the handle surface and some minor vibration of the mirror.

As also shown in Fig. 6, while the phase angles measured with the 1-D laser were basically in the range of $\pm 5^\circ$, the phase angles measured with the 3-D laser vibrometer generally decreased with the increase in the frequency. To further identify the source of the phase difference, an adapter equipped with a tri-axial accelerometer was firmly attached to the handle to measure its surface transmissibility. The results further confirmed that the magnitudes measured with the 3-D laser vibrometer are acceptable, and that the differences in the measured phase were not caused by the handle response, but believed to be an issue related to the signal processing in the 3-D vibrometer. Fortunately, such a phase difference does not vary with time and measurement location; therefore it can be corrected using Eq. (3). The correction can also largely take care of the non-unity magnitude response shown in Fig. 6, similar to the method required to correct the transmissibility in the standardized glove test (ISO 10819, 1996). The 3-D results described in the following are all results corrected by using Eq. (3) and the 3-D handle

transmissibility data (T_{Handle}) shown in Fig. 6, unless specifically mentioned otherwise.

As a further check-up test, the 1-D laser vibrometer was also used to measure the vibration transfer function in the X direction on one of the subjects in the proximal area shown in the Fig. 4. The comparisons are shown in Fig. 7. The transfer functions measured with these two vibrometers were very comparable, in terms of both magnitude and phase angle. Because the 3-D and 1-D tests were carried out on two different days, the hand and arm postures, applied hand forces, and measurement points were unlikely to be exactly the same. These possible differences, however, did not substantially affect the results.

3.2. Vibration transmissibility on the fingers

Fig. 8 shows the mean transfer functions of the subjects at the first six points in the proximal area on the fingers illustrated in Fig. 4. As expected, the transmissibility generally varied with the vibration direction ($p < 0.001$) and the specific location ($p < 0.001$). Their interaction was also significant ($p < 0.001$). However, the basic trends of the transmissibility in the frequency domain at a similar location on the fingers are similar. As also expected, the magnitude of the transmissibility at each point in each direction was close to unity at low frequencies (< 25 Hz), and the corresponding phase angle was

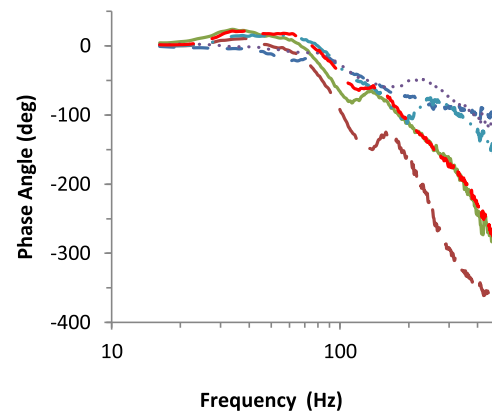
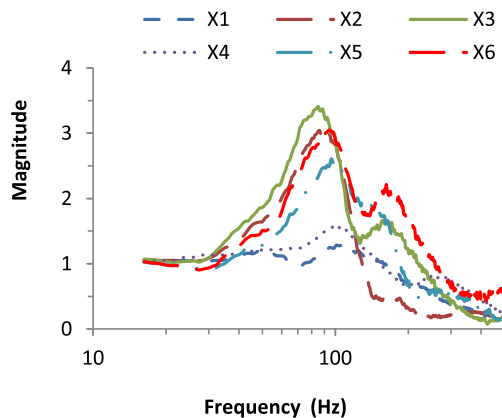
close to zero. The magnitude generally increased with the frequency before it reached a resonant peak frequency, which varied with the vibration direction and measuring location. While the resonance magnitude in the Z direction was the lowest, the highest resonance magnitude was in the Y direction.

Fig. 9 shows the mean transmissibility functions of the subjects at the remaining five points (P7–P11) in the fingertip area illustrated in Fig. 4. Similar to those observed in Fig. 8, the transmissibility depended on the location ($p < 0.001$) and vibration direction ($p < 0.001$). Their interaction was also significant ($p < 0.001$). Although the peak transmissibility values at the fingertip (P8) were less than those at some other locations, its transmissibility values were generally at a high level ($Tr > 1.0$) in a large frequency range, especially in the Y and Z directions. Some of the transmissibility values at high frequencies (> 250 Hz) (e.g., P9 and P11 in X direction) were very low; therefore, the corresponding measured phase angles are probably not accurate.

3.3. Vibration transmissibility on the hand dorsum

Figs. 10 and 11 show the mean transmissibility functions of the subjects on the hand dorsum (Fig. 5). The effects of the vibration direction ($p < 0.001$) and the specific location ($p < 0.001$) were significant, but their interaction was not significant ($p = 0.750$).

(a) 3-D laser vibrometer



(b) 1-D laser vibrometer

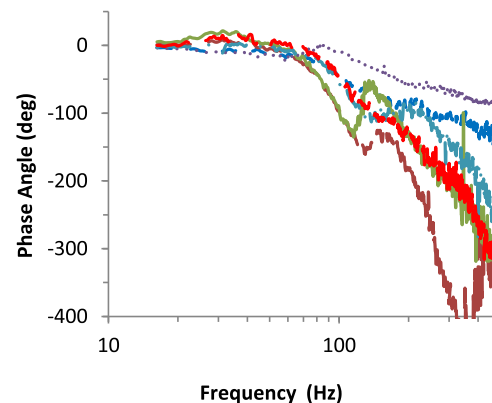
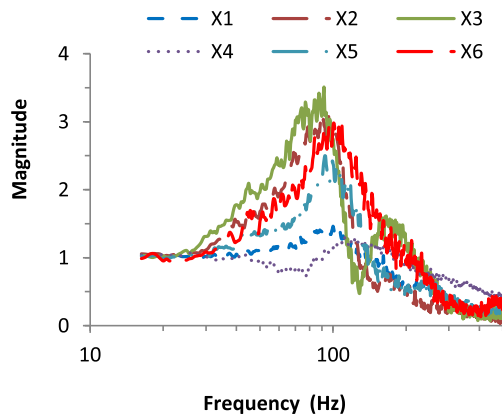


Fig. 7. Comparisons of the vibration transmissibility functions measured using the 3-D and 1-D laser vibrometers on one subject at Points 1–6 in the proximal area on the index and middle fingers in the x_h direction shown in Fig. 4.

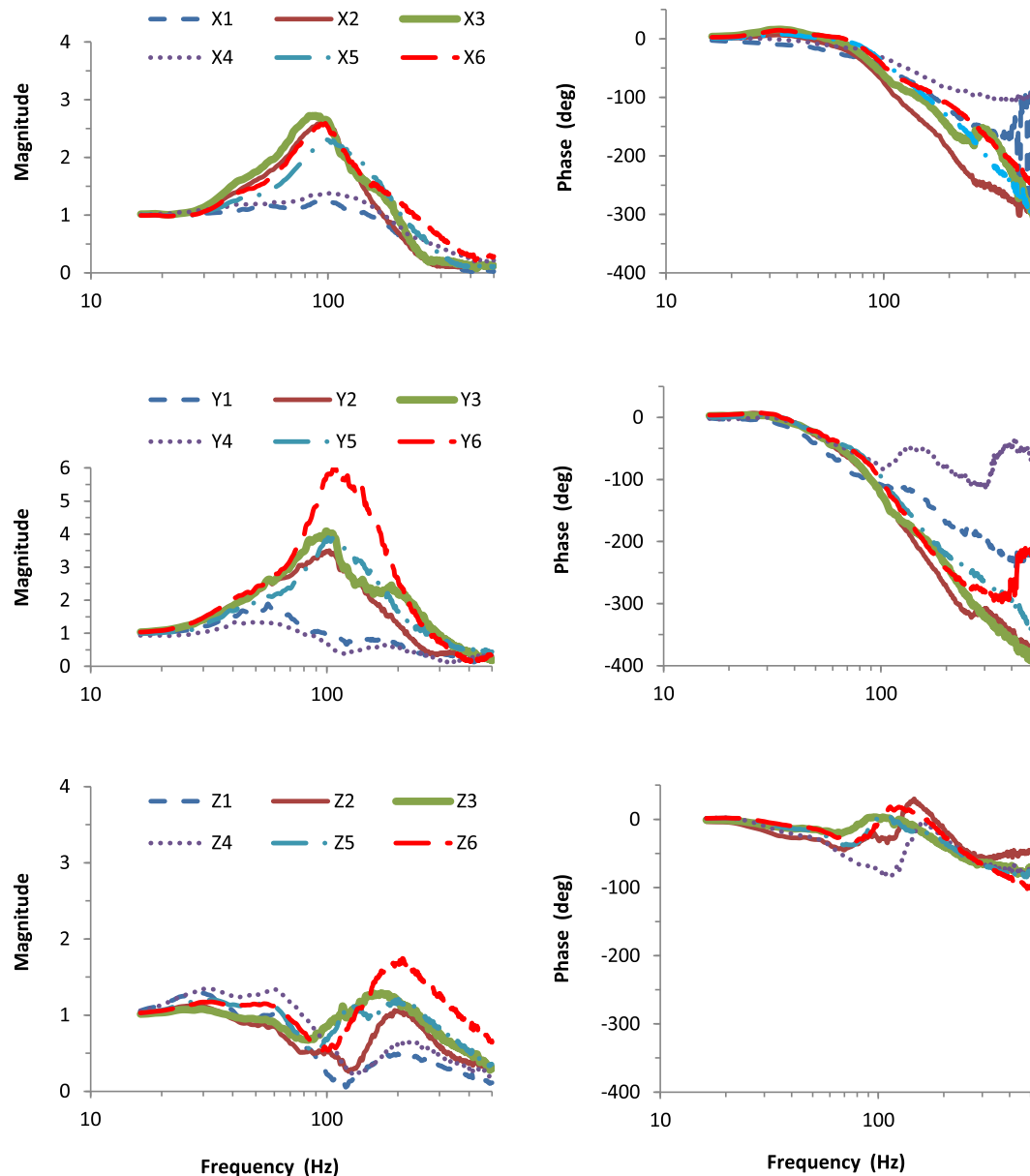


Fig. 8. Mean vibration transmissibility functions of the subjects in each direction at Points 1–6 in the proximal area on the index and middle fingers shown in Fig. 4.

Their differences in each direction were also less than those observed on the fingers shown in Figs. 8 and 9. Similar to those observed in Figs. 8 and 9, the transmissibility in the Z direction was generally the lowest one, and that in the Y direction was generally the highest at each measuring point. Again, when the transmissibility value became small, the phase angle might not be reliable due to possible measurement errors at high frequencies where the transmissibility magnitudes were low.

3.4. Vibration transmissibility on the wrist-forearm-elbow substructure

Fig. 12 shows the mean transmissibility functions of the subjects at the ten points (P10–P19) on the wrist-forearm-elbow substructure (Fig. 3). The transmissibility of the vibration at greater than 100 Hz was less than 20%, except that at P18 and P19 on the wrist in the Y direction. From 16 to 100 Hz, the effects of the vibration direction ($p < 0.001$) and the location ($p < 0.001$) on the transmissibility and their interaction were significant ($p < 0.001$).

Specifically, the highest peak transmissibility was also observed in the Y direction, but the differences among the transmissibility values at each point in the three directions were not as large as those on the hand. The transmissibility generally decreased with the increase in distance from the hand, except at P10, which was in the bony area of the elbow. The transmissibility functions at P18 and P19 (Fig. 3) were similar to those at P10 and P11 (Fig. 5) measured in the hand dorsum test. This is because these points were at similar locations near the wrist, although the wrist and arm postures used in the test were not the same.

3.5. Vibration transmissibility on the upper arm

Fig. 13 shows the mean transmissibility functions of the subjects at the nine points (P1–P9) on the upper arm (Fig. 3). The transmissibility of the vibration at greater than 60 Hz was generally less than 10%. From 16 to 60 Hz, the effects of the vibration direction ($p < 0.001$) and the location ($p < 0.001$) on the transmissibility were significant, but their interaction was not significant ($p = 0.977$).

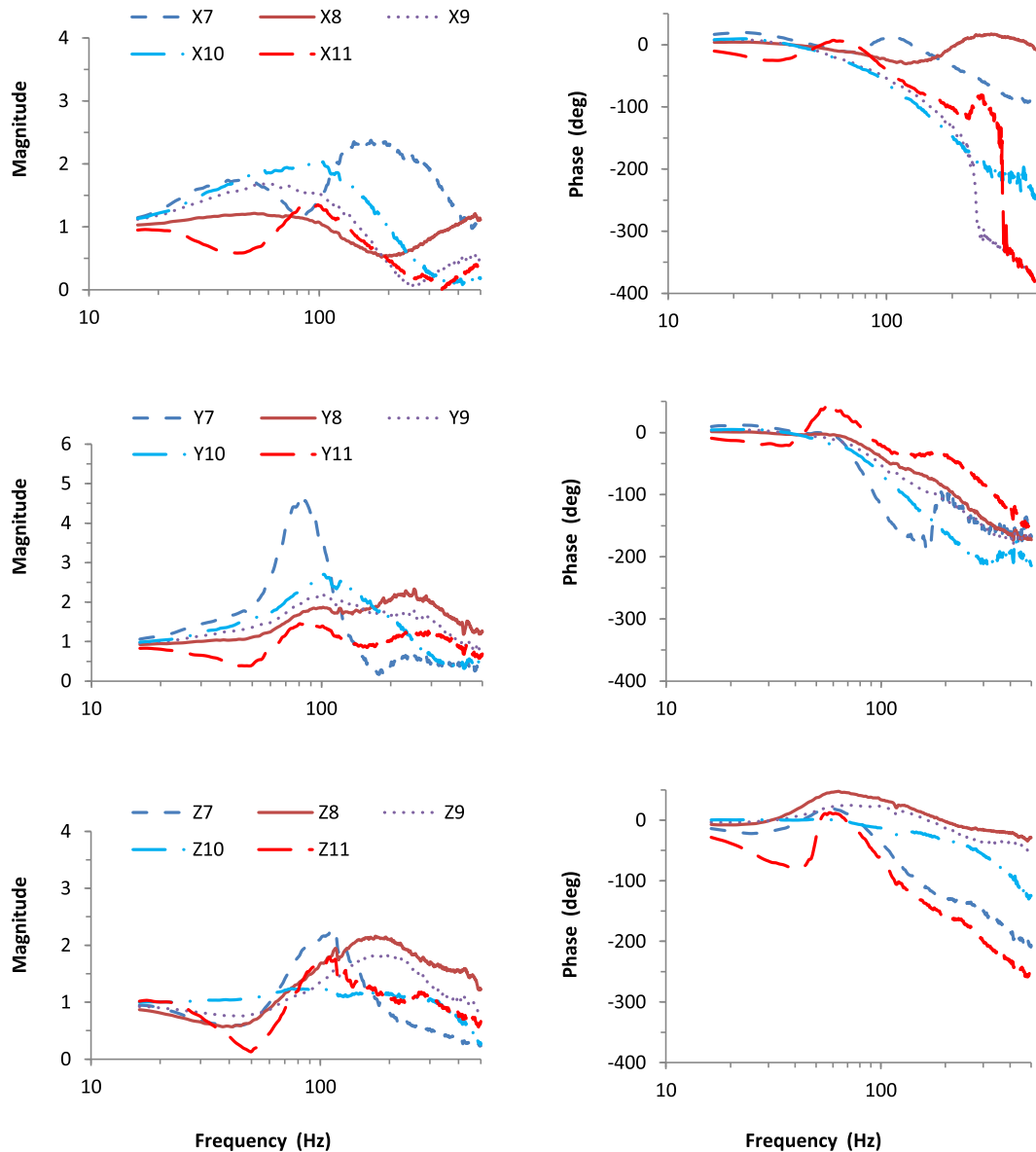


Fig. 9. Mean vibration transmissibility functions of the subjects in each direction at Points 7–11 in the fingertip area on the index and middle fingers shown in Fig. 4.

Specifically, the transmissibility at the distal parts of the upper arm (P6–P9) was generally greater than that at the parts close to the shoulder. The maximum transmissibility near the shoulder (P1–P5) in each direction was less than 30%, which could be higher at frequencies below 16 Hz, but it was not measured in this study.

4. Discussions

This study used a new technology to measure the 3-D vibrations on the hand-arm system. The results provide useful information for enhancing the understanding of the basic biodynamic characteristics of the system and they may be used for the further development of the hand-arm system model.

4.1. Advantages and limitations of the 3-D scanning laser vibrometer

As shown in Figs. 6 and 7, the results of this study suggest that the 3-D laser vibrometer can provide a reasonable measurement of

the vibration transmitted to the hand-arm system in the frequency range at least up to 250 Hz. Obviously, this technology can increase the efficiency of the measurement. While it is very difficult to measure the vibrations in the tangential directions of the skin surface using a single-axis vibrometer, the 3-D technology can overcome this difficulty. The simultaneous measurements of the vibrations in the three directions may also make it easier to identify and analyze the coupling effects.

This study also revealed that the 3-D laser vibrometer has some technical limitations. This study identified a phase-shift problem, as shown in Fig. 6. It is necessary to correct it using Eq. (3). This finding has also helped improve the data processing program of the vibrometer to substantially reduce the shift, as confirmed in a follow-up study (Welcome et al., 2014). A major remaining difficulty is to focus the three laser beams at the same point during the measurement due to the difficulty of maintaining a stable position of the hand-arm during the entire experiment for each subject. If the laser beams are reflected from different points on the skin, they cannot provide consistent information to accurately determine the

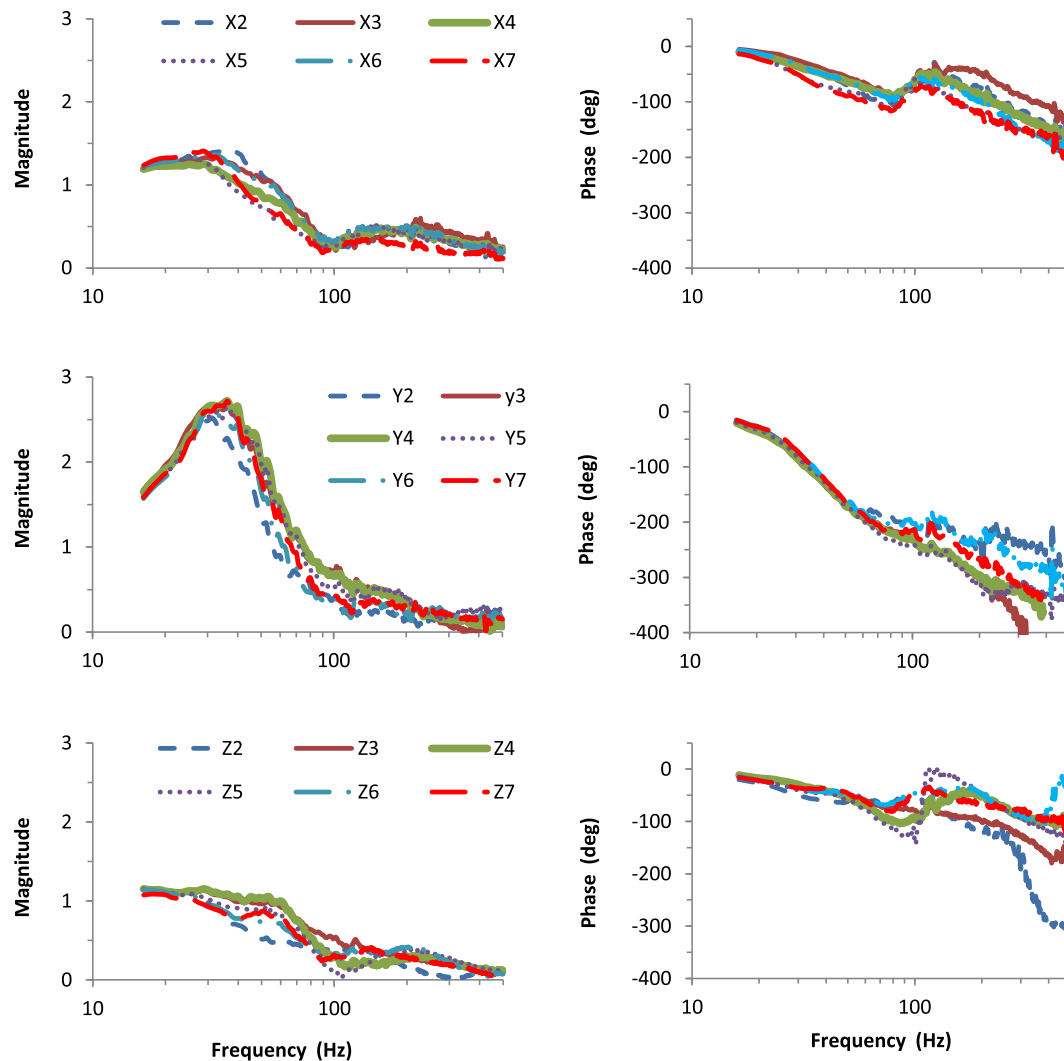


Fig. 10. Mean vibration transmissibility functions of the subjects in each direction at Points 2–7 on the hand dorsum shown in Fig. 5.

vibration in each direction. This may become a critical issue for measuring high-frequency responses, as the local vibration may vary sensitively with the specific location of the skin. As the subject can only maintain a stable position and hand force for a short period of time, reducing the number of scanning points in each trial may reduce the uncertainty of the laser focus. This, however, will reduce the efficiency and increase the expense of the measurement.

4.2. Effects of location and direction

The results of this study confirm that while vibrations at lower than 25 Hz can be effectively transmitted to the arms and shoulder, transmission of vibrations at higher frequencies (>50 Hz) are primarily limited to the hand or fingers, which are qualitatively consistent with the findings reported in other studies (Pyökö et al., 1976; Reynolds, 1977). As shown in Fig. 9, the vibration can be effectively transmitted ($T_r \geq 1.0$) to the fingertip areas (P8 and P9 in Fig. 5) at more than 300 Hz in some vibration directions. This is also consistent with the findings reported before (Sörensson and Lundström, 1992). The high transmissibility results are likely due to the following reasons: (a) the mass per unit length at this part of the finger is the smallest; (b) the contact stiffness per unit length at the fingertip is likely to be higher than that at other locations due to the largest contact pressure at the

fingertip in a power grip on a cylindrical handle for the vast majority of the subjects (Chao et al., 1989; Aldien et al., 2005); and (c) there is no constraint at the end of the fingertip.

Because of the changes of these three factors, the frequency range of the effective transmissibility and the resonant frequencies at the remaining parts of the fingers are generally smaller than that at the fingertip, as shown in Fig. 8. However, their resonant magnitudes, especially at the proximal/third phalangeal dorsum (P2, P3, P5, and P6 in Fig. 4), were higher. This is largely because the contact pressure at this part of the fingers could be generally smaller than that at the fingertip and that at the distal phalanx; as a result, each finger is structurally like a small bridge with one base anchored at the proximal phalanx and another one at the distal palm.

As shown in Figs. 10 and 11, the effective vibration transmission ($T_r \geq 1.0$) on the hand dorsum was generally limited to the range lower than 80 Hz with resonant frequencies in the neighborhood of 35 Hz. This is partially because the effective mass of the palm-hand dorsal substructure is larger than that of the fingers. Also, this substructure is directly constrained by the wrist-arm substructure, and partially the overall palm contact stiffness is generally much less than that at the fingers (Aldien et al., 2005). Unlike the transfer functions at other parts of the hand-arm system, the transfer functions on the hand dorsum did not vary

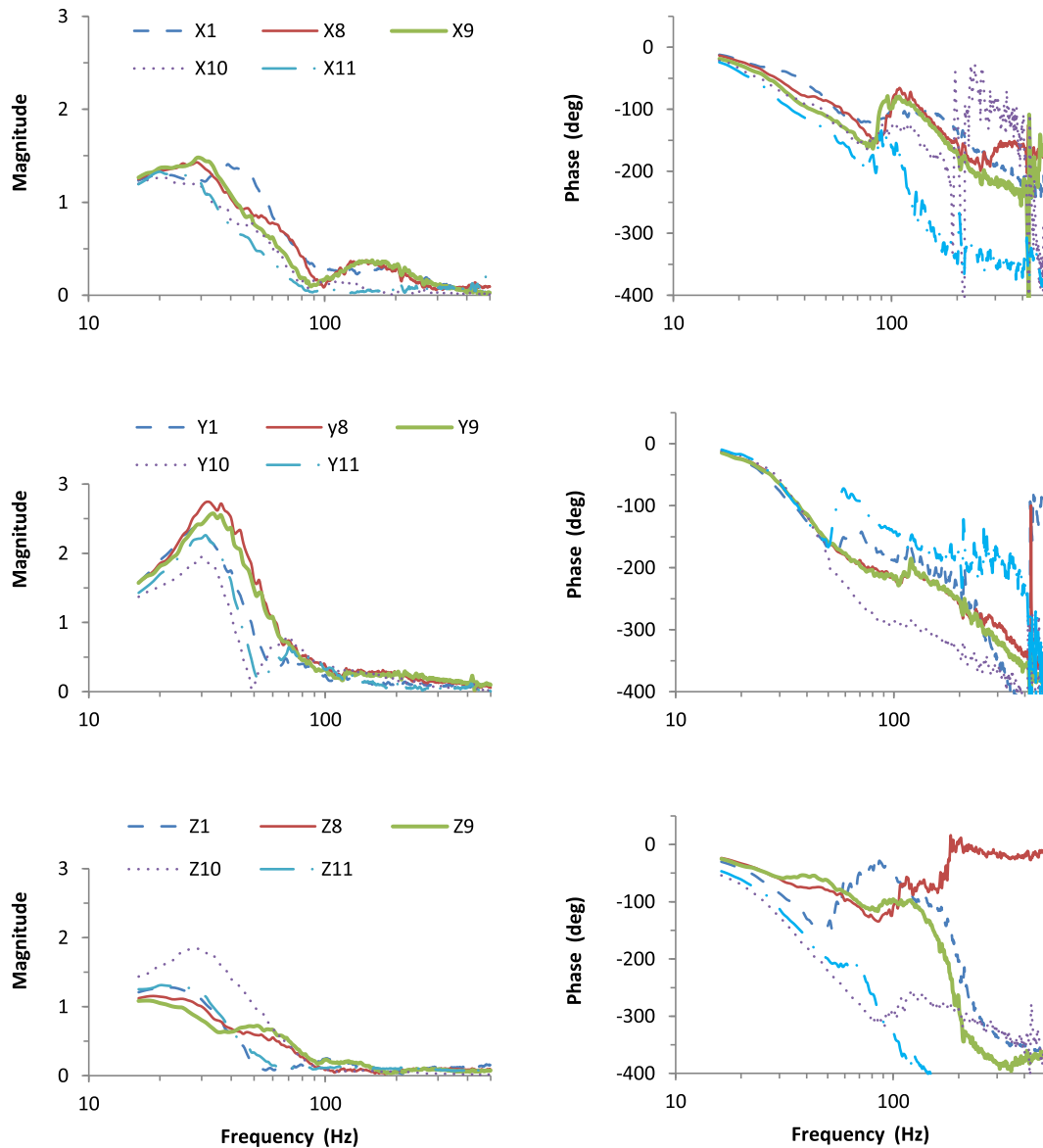


Fig. 11. Mean vibration transmissibility functions of the subjects in each direction at Points 1 and 8–11 on the hand dorsum shown in Fig. 5.

substantially, especially in the X and Y directions. This suggests that the dynamic properties on this substructure with the posture used in the experiment are fairly evenly distributed. This may also explain why the interaction between the direction and position for the transmissibility measured on the hand dorsum was not significant. Probably for the same reason, no significant direction–position interaction for the upper arm transmissibility was observed. On the other hand, the significant interaction observed in the transmissibility data measured on the fingers and forearm may suggest that the dynamic properties of these substructures vary significantly with both direction and location. The non-significant interaction for the transmissibility measured on the upper arm needs further verification, as the frequency range used in this study (16–500 Hz) does not cover the major resonant frequency of the upper arm (8–12 Hz) (Kinne et al., 2001; Dong et al., 2007; Adewusi et al., 2012).

While the vibration at a specific location on the hand results from the responses to both the local excitation in the contact area and the vibration transmitted from other parts of the hand, the arm

response results solely from the vibration transmitted from the hand. As expected, the transmissibility on the wrist–arm substructure is generally reduced with the increase in the distance from the hand, as shown in Figs. 12 and 13. However, some exceptions were also observed in this study. The first exception is that the transmissibility measured at the bony area of the elbow (P10) was generally greater than that at many other points on the arms, as shown in Fig. 12. This is because the hand–arm system is not a uniform medium. The bones in the system must be much stiffer and less damped than the soft tissues and the vibration must transfer more effectively along the bones in each direction. Because the joint tissues in their translational directions are also much more rigid than the other soft tissues in the system, these joints must be able to transmit the translational vibrations more effectively than the soft tissues. This theory can also explain why the transmissibility at the elbow along the forearm direction could be similar to that measured at the wrist if the accelerometer is firmly attached to the bony area of the elbow, as reported in other studies (Reynolds, 1977; Pyykkö et al., 1976).

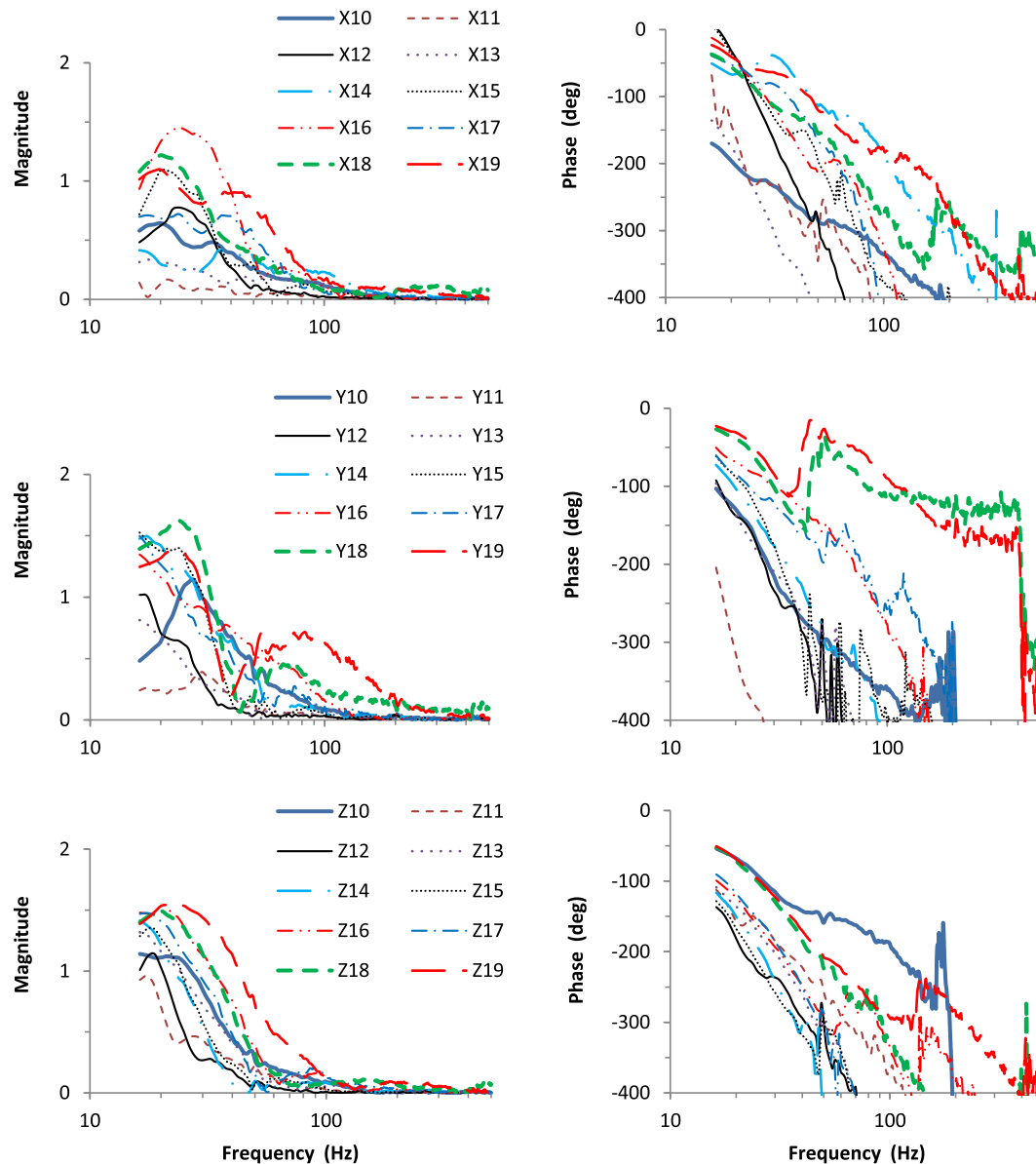


Fig. 12. Mean vibration transmissibility functions of the subjects in each direction at the ten points (P10–P19) on the wrist-forearm-elbow substructure illustrated in Fig. 3.

The second exception is that the transmissibility measured at the same cross-sectional location on the arm could be significantly different at some frequencies, as shown in Figs. 12 and 13. This may partially result from measurement errors and partially result from the resonant response of the local substructure. The boney and soft tissues may form a local dynamic system, and its resonance may play a dominant role in determining the transmissibility in a certain frequency range.

4.3. Implications of the results for risk assessment

As the first degree of approximation, the vibration transmissibility may be used as a location-specific biodynamic frequency weighting (Thomas and Beauchamp, 1998; Dong et al., 2005b; Wu et al., 2010). The fundamental vibration frequencies of many tools such as chipping hammers, rock drills, and rivet hammers are in the range of 25–40 Hz (Griffin, 1997). The results of this study indicate that the resonances of the hand dorsum-wrist-

forearm substructures in the three directions are also in this frequency range. This is consistent with the finding from a driving-point biodynamic response study (Dong et al., 2012). This coincidence may be one of the major mechanisms of the vibration or shock-induced wrist and elbow injuries and disorders (Bovenzi et al., 1987; Gemme and Saraste, 1987).

The results of this study also indicate that the finger resonances in the three directions are at more than 50 Hz, primarily in the range of 80–250 Hz. Therefore, the high biodynamic frequency weightings should be in this frequency range. The frequency weighting function defined in the current standard largely emphasizes frequencies below 50 Hz (ISO 5349-1, 2001); therefore, the current weighting function is very likely to be unsuitable for assessing the finger disorders. The dominant vibration frequencies of many tools such as grinders, chainsaws, impact wrenches, and orbital sanders are in the range of 80–160 Hz. Such vibration exposures are thus likely to be primarily associated with finger or hand disorders but the current frequency weighting is likely to

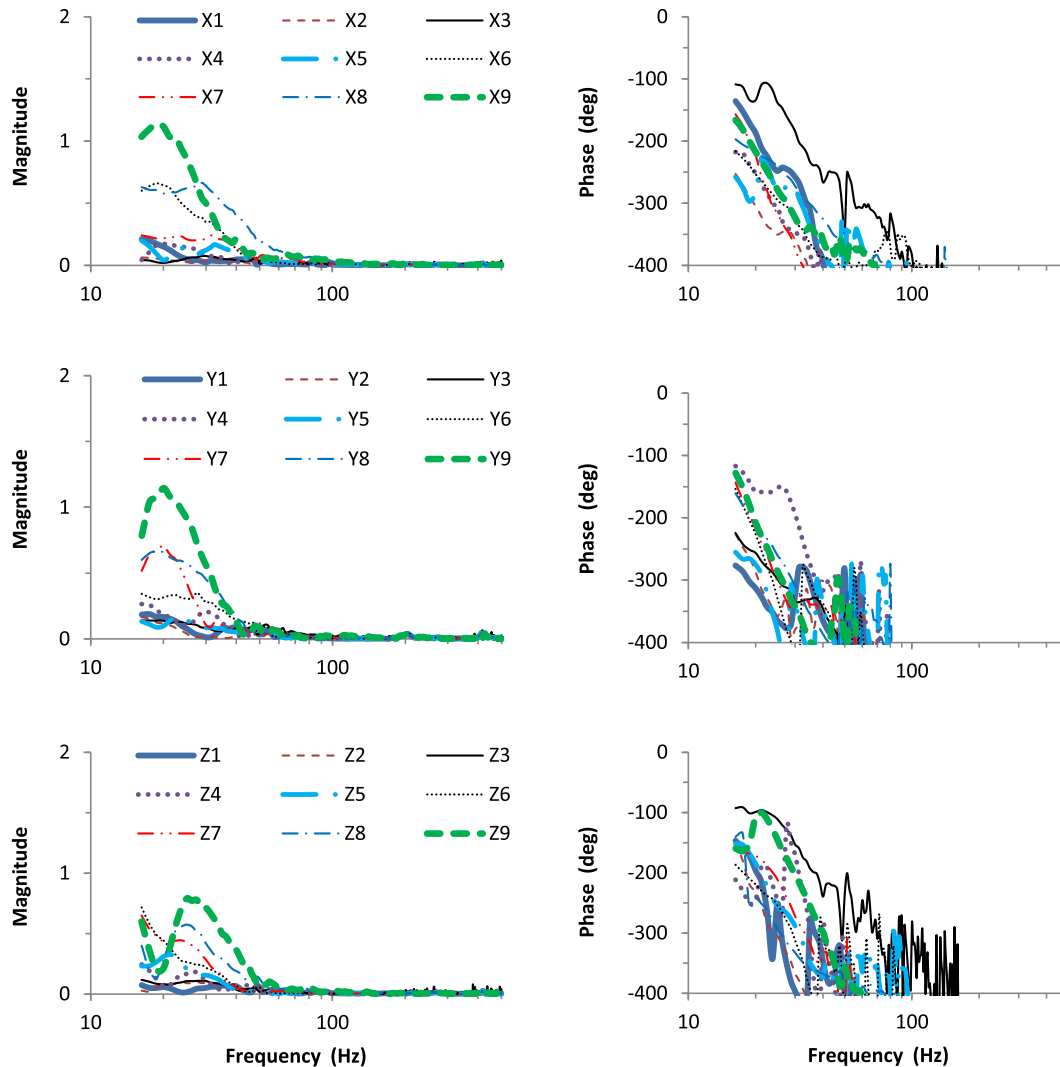


Fig. 13. Mean vibration transmissibility functions of the subjects in each direction at the nine points (P9–P19) on the upper arm illustrated in Fig. 3.

underestimate the effects of the vibration at such frequencies. This prediction is consistent with the findings of health effect studies (Barregard et al., 2003; Tominaga, 1993, 2005).

This study also found that the highest transmissibility to the hand is in the Y direction. This means a higher dynamic deformation of the hand soft tissues or a higher biodynamic frequency weighting in this direction. However, this may not necessarily translate to a higher risk of injury in this direction because the frequency dependency of any injury or disorder depends not only on the biodynamic weighting but also on the biological weighting (Griffin, 1990; Dong et al., 2005a). That is, the human hand and fingers may have been naturally built or evolved to have a higher threshold of injury in this direction. This may be a good hypothesis for further studies.

4.4. Implications of the results for the simulation of the hand-arm system

The spatial changes of vibration transmissibility observed in this study suggest that it is generally difficult to create a reliable model based on the transfer functions measured at one or two points on each substructure of the system to represent the biodynamic properties of the system and to predict the distributed biodynamic

responses. This study provides spatial transfer functions on the entire hand-arm system in the three directions. They may be used to help develop more comprehensive 3D models of the hand-arm system.

5. Conclusions

To enhance the understanding of the vibration transmission in the hand-arm system, a 3-D laser vibrometer was used to measure the vibration transmitted to the system in three orthogonal directions. The results of the study confirm that the vibration transfer function depends on the vibration direction and the measurement location. The magnitude of the resonance and its peak frequency also largely depend on the location and direction. For hand and arm postures and the hand coupling condition (30 N grip and 50 N push) used in the experiment, the vibration was effectively transmitted ($Tr > 1.0$) to fingertip at frequencies above 300 Hz in some cases. On the other hand, only part of the vibration at less than 50 Hz ($Tr < 0.5$) was transmitted to the majority of locations on the upper arm and shoulder. On the fingers, a major resonance was observed at around 100 Hz in the X and Y directions and around 200 Hz in the Z direction. The major resonance on the hand dorsum and wrist occurred at around 30–40 Hz in each direction. These

observations suggest that the current frequency weighting that emphasizes vibrations at less than 25 Hz may not be suitable for assessing the risk of the hand, especially the fingers in the vibration exposure. This study also found that the resonance magnitude on the fingers and hand dorsum in the Z direction was generally the lowest and that the resonance amplitude in the Y direction was generally the highest. The transmissibility on the forearm-elbow-upper arm generally reduced with the increase in distance from the hand. The measured transfer functions on the entire hand-arm system in the three directions may also be useful for developing more comprehensive models of the hand-arm system to help further understand and assess the vibration-induced disorders.

Disclaimers

The content of this publication does not necessarily reflect the views or policies of the National Institute for Occupational Safety and Health (NIOSH), nor does mention of trade names, commercial products, or organizations imply endorsement by the U.S. Government.

References

Adeyemi, S.A., Rakheja, S., Marcotte, P., 2012. Biomechanical models of the human hand-arm to simulate distributed biodynamic responses for different postures. *Int. J. Ind. Ergon.* 42, 249–260.

Aldien, Y., Welcome, D.E., Rakheja, S., Dong, R.G., Boileau, P.-E., 2005. Contact pressure distribution at hand-handle interface: role of hand forces and handle size. *Int. J. Ind. Ergon.* 35, 267–286.

Barregard, L., Ehrenström, L., Marcus, K., 2003. Hand-arm vibration syndrome in Swedish car mechanics. *Occup. Environ. Med.* 60, 287–294.

Bovenzi, M., Fiorito, A., Volpe, C., 1987. Bone and joint disorders in the upper extremities of chipping and grinding operations. *Int. Arch. Occup. Environ. Health* 59, 189–198.

Chao, E.Y.S., An, K.N., Cooney III, W.P., Linscheid, R.L., 1989. Chapter 5: Hand Functional Strength Assessment and its Clinical Application. *Biomechanics of the Hand*, World Scientific, London.

Cherian, S., Rakheja, S., Bhat, R.B., 1996. An analytical investigation of an energy flow divider to attenuate hand-transmitted vibration. *Int. J. Ind. Ergon.* 17, 455–467.

Concettoni, E., Griffin, M., 2009. The apparent mass and mechanical impedance of the hand and the transmission of vibration to the fingers, hand, and arm. *J. Sound Vib.* 325 (3), 664–678.

Deboli, R., Miccoli, G., Rossi, G.L., 1999. Human hand-transmitted vibration measurements on pedestrian controlled tractor operators by a laser scanning vibrometer. *Ergonomics* 42 (6), 880–888.

Dong, R.G., Wu, J.Z., Welcome, D.E., 2005a. Recent advances in biodynamics of hand-arm system. *Ind. Health* 43, 449–471.

Dong, R.G., Welcome, D.E., Wu, J.Z., 2005b. Frequency weightings based on biodynamics of fingers-hand-arm system. *Ind. Health* 43, 485–494.

Dong, R.G., Dong, J.H., Wu, J.Z., Rakheja, S., 2007. Modeling of biodynamic responses distributed at the fingers and the palm of the human hand-arm system. *J. Biomech.* 40, 2335–2340.

Dong, R.G., Welcome, D.E., McDowell, T.W., Wu, J.Z., 2013. Theoretical relationship between vibration transmissibility and driving-point response functions of the human body. *J. Sound Vib.* 332 (24), 6193–6202.

Dong, R.G., Welcome, D.E., Xu, X.S., Warren, C., McDowell, T.W., Wu, J.Z., Rakheja, S., 2012. Mechanical impedances distributed at the fingers and Palm of the human hand in three orthogonal directions. *J. Sound Vib.* 331, 1191–1206.

Gemme, G., Saraste, H., 1987. Bone and joint pathology in workers using hand-held vibration tools. *Scand. J. Work, Environ. Health* 13, 290–300.

Giacomin, J., Shaya, M.S., Dormegnien, E., Richard, L., 2004. Frequency weighting for the evaluation of steering wheel rotational vibration. *Int. J. Ind. Ergon.* 33, 527–541.

Griffin, M.J., 1990. *Handbook of Human Vibration*. Academic Press, London.

Griffin, M.J., 1994. Foundations of hand-transmitted vibration standards. *Nagoya J. Med. Sci.* 57 (Suppl.), 147–164.

Griffin, M.J., Macfarlane, C.R., Norman, C.D., 1982. The transmission of vibration to the hand and the influence of Gloves. In: Brammer, A.J., Taylor, W. (Eds.), *Vibration Effects on the Hand and Arm in Industry*. John Wiley & Sons, New York, pp. 103–116.

Griffin, M.J., 1997. Measurement, evaluation, and assessment of occupational exposures to hand-transmitted vibration. *Occup. Environ. Med.* 54 (2), 73–89.

Gurram, R., Rakheja, S., Gouw, G.J., 1994. Vibration transmission characteristics of the human hand-arm system and gloves. *Int. J. Ind. Ergon.* 13 (3), 217–234.

ISO 5349-1, 2001. Mechanical Vibration- Measurement and Evaluation of Human Exposure to Hand-transmitted Vibration – Part 1: General Guidelines. International Organization of Standard, Geneva, Switzerland.

ISO 10819, 1996. Mechanical Vibration and Shock – Hand-arm Vibration – Method for the Measurement and Evaluation of the Vibration Transmissibility of Gloves at the Palm of the Hand. International Organization of Standard, Geneva, Switzerland.

ISO-10068, 1998. Mechanical Vibration and Shock – Free, Mechanical Impedance of the Human Hand-arm System at the Driving Point. International Organization of Standard, Geneva, Switzerland.

Kihlberg, S., Attebrant, M., Gemne, G., Kjellberg, A., 1995. Acute effects of vibration from a chipping hammer and a grinder on the hand arm system. *Occup. Environ. Med.* 52, 731–737.

Kinne, J., Latzel, K., Schenk, T.H., 2001. Application of two-hand impedance as basis for mechanical modeling. In: *Proceedings of the 9th International Conference on Hand-arm Vibration 2001*, Nancy, France, pp. 113–118.

McDowell, T.W., Kashon, M.L., Welcome, D.E., Warren, C., Dong, R.G., 2007. Relationships between psychometrics, exposure conditions, and vibration power absorption in the hand-arm system. In: *Proceedings of the 11th International Conference on Hand-arm Vibration*, Bologna, Italy.

Miwa, T., 1968. Evaluation methods for vibration effects. Part 4: measurement of vibration greatness for whole body and hand in vertical and horizontal vibration. *Ind. Health* 6, 1–10.

Morioka, M., Griffin, M.J., 2006. Magnitude-dependence of equivalent comfort contours for fore-and-aft, lateral and vertical hand-transmitted vibration. *J. Sound Vib.* 295, 633–648.

Nataletti, P., Paonez, N., Scalise, L., 2005. Measurement of hand-vibration transmissibility by non-contact measurement techniques. In: *International Conference on Environmental Health Risk*, Bologna, Italy, pp. 315–324.

NIOSH, 1997. Musculoskeletal Disorders and Workplace Factors - a Critical Review of Epidemiological Evidence for Work-related Musculoskeletal Disorders of the Neck, Upper Extremity, and Low Back. DHHS (NIOSH). Publication No. 97–141.

Pyykkö, I., Färkkilä, M., Toivanen, J., Korhonen, O., Hyvärinen, J., 1976. Transmission of vibration in the hand-arm system with special reference to changes in compression force and acceleration. *Scand. J. Work, Environ. Health* 2, 87–95.

Reynolds, D.D., 1977. Hand-Arm Vibration: a review of 3 years' research. In: Wasserman, D.E., Taylor (Eds.), *Proceedings of the International Occupational Hand-arm Vibration Conference*, Cincinnati, Ohio, USA. National Institute for Occupational Safety and Health, pp. 99–128.

Rossi, G.L., Tomasini, E.P., 1995. Hand-arm vibration measurement by a laser scanning vibrometer. *Measurement* 16 (22), 113–124.

Sakakibara, H., Kondo, T., Miyao, M., Yamada, S., Nakagawa, T., Kobayashi, F., Ono, Y., 1986. Transmission of hand-arm vibration to the head. *Scand. J. Work Environ. Health* 359–361.

Scalise, L., Rossetti, F., Paone, N., 2007. Hand vibration: non-contact measurement of local transmissibility. *Int. Arch. Occup. Environ. Health* 81, 31–40.

Sörensson, A., Lundström, R., 1992. Transmission of vibration to the hand. *J. Low Freq. Noise Vib.* 11, 14–22.

Thomas, M., Beauchamp, Y., 1998. Development of a new frequency weighting filter for the assessment of grinder exposure to wrist transmitted vibration. *Comput. Ind. Eng.* 35 (3–4), 651–654.

Tominaga, Y., 1993. The relationship between vibration exposure and symptoms of vibration syndrome. *J. Sci. Labor* 1–14.

Tominaga, Y., 2005. New frequency weighting of hand-arm vibration. *Ind. Health* 43, 509–515.

Welcome, D.E., Dong, R.G., Xu, X.S., Warren, C., McDowell, T.W., Wu, J.Z., 2011. An investigation on the 3-D vibration transmissibility on the human hand-arm system using a 3-D scanning laser vibrometer. *Can. Acoust.* 39 (2), 44–45.

Welcome, D.E., Dong, R.G., Xu, X.S., Warren, C., McDowell, T.W., 2014. The effects of vibration-reducing gloves on finger vibration. *Int. J. Ind. Ergon.* 44, 45–59.

Wu, J.Z., Dong, R.G., Welcome, D.E., Xu, X.S., 2010. A method for analyzing vibration power absorption density in human fingertip. *J. Sound Vib.* 329, 5600–5614.

Xu, X.S., Welcome, D.E., McDowell, T.W., Wu, J.Z., Warren, C., Dong, R.G., 2011. The vibration transmissibility and driving-point biodynamic response of the hand exposed to vibration normal to the palm. *Int. J. Ind. Ergon.* 41 (5), 418–427.